Wave dissipation by muddy seafloors

Steve Elgar[1] and Britt Raubenheimer[1]

Received 10 January 2008; revised 19 February 2008; accepted 4 March 2008; published 12 April 2008.

[1] Muddy seafloors cause tremendous dissipation of ocean waves. Here, observations and numerical simulations of waves propagating between 5- and 2-m water depths across the muddy Louisiana continental shelf are used to estimate a frequency- and depth-dependent dissipation rate function. Short-period sea (4 s) and swell (7 s) waves are shown to transfer energy to long-period (14 s) infragravity waves, where, in contrast with theories for fluid mud, the observed dissipation rates are highest. The nonlinear energy transfers are most rapid in shallow water, consistent with the unexpected strong increase of the dissipation rate with decreasing depth. These new results may explain why the southwest coast of India offers protection for fishing (and for the 15th century Portuguese fleet) only after large waves and strong currents at the start of the monsoon move nearshore mud banks from about 5- to 2-m water depth. When used with a numerical nonlinear wave model, the new dissipation rate function accurately simulates the large reduction in wave energy observed in the Gulf of Mexico. **Citation:** Elgar, S., and B. Raubenheimer (2008), Wave dissipation by muddy seafloors, *Geophys. Res. Lett.*, *35*, L07611, doi:10.1029/2008GL033245.

1. Introduction

[2] Muddy seafloors are ubiquitous on the world's continental shelves, and cause strong dissipation of ocean surface-gravity waves [*Gade*, 1958; *Wells and Coleman*, 1981; *Mathew et al.*, 1995; *Sheremet and Stone*, 2003], protecting coastal areas from storms and tsunamis. The arrival of mud banks in the shallow waters off the southwest coast of India are welcomed in a celebration known as "Chakara" because the damping of the large monsoon-driven waves results in calm waters onshore of the mud banks that allow the yearly harvest of fish [*Nair*, 1988; *Jiang and Mehta*, 1996]. The calm waters onshore of the Kerala mud banks also provided safe harbor for Vasco deGamma during the monsoons of 1498 [*Pazhama*, 1996]. Strong dissipation of waves propagating over muddy seafloors also has been observed near the coast of Surinam [*Wells and Coleman*, 1981; *Wintertwerp et al.*, 2007], in the Gulf of Mexico [*Forristall and Reece*, 1985; *Sheremet and Stone*, 2003], and in laboratories [*Gade*, 1958; *Kaihatu et al.*, 2007].

[3] There are many theories for dissipation of surface waves owing to interactions with a layer of mud near the seafloor. Differences between the corresponding dissipation-rate functions are owing to different assumptions about the rheology of the sediment, which include combinations of elastic, plastic, viscous, and porous media [e.g., *Gade*, 1958; *Mei and Liu*, 1973; *Dalrymple and Liu*, 1978; *Yamamoto et al.*, 1978; *MacPherson*, 1980; *Hsiao and Shemdin*, 1980; *Mei and Liu*, 1987; *Liu and Mei*, 1989; *Jiang and Mehta*, 1995, 1996; *Ng*, 2000; *Lee et al.*, 2002]. The theoretical dissipation rates, which depend on sediment properties (e.g., density, viscosity, shear modulus), mud-layer thickness, water depth, and wave period or wavelength, have been shown to be consistent with laboratory studies of waves propagating in a two-layer fluid [*Gade*, 1958; *Kaihatu et al.*, 2007]. Some of the theoretical dissipation-rate functions have been incorporated into numerical wave models, with mixed success when compared with field observations [*Wintertwerp et al.*, 2007].

[4] Although mud-induced dissipation of ocean surface gravity waves is important on many continental shelves, there are no observation-based estimates of the dissipation rate function. Here, observations of waves propagating 1.8 km across the Louisiana continental shelf (Figure 1) are used to estimate the frequency- and depth-dependent mud-induced dissipation rate function.

2. Field Observations

[5] Mud is advected into the area by the Atchafalaya and Mississippi Rivers, and settles onto the seafloor [*Allison et al.*, 2000; *Draut et al.*, 2005]. SCUBA divers observed an approximately 0.3-m thick layer of yogurt-like mud above a harder clay bottom. Shipboard measurements along the instrumented transect indicate the near-bottom mud had a density of approximately 1.3 g/cm^3 (G. Kineke, personal communication, 2007), and had sufficient shear strength that it was recovered in clamshell box cores, implying the mud was not fluid. Colocated pressure gages and current meters were deployed approximately 0.75 m above the seafloor between 5- and 2-m water depths for 24 days in Mar-Apr 2007 (Figure 1).

[6] Overall energy flux (F, defined here as the wave energy times the group velocity integrated over the frequency band $0.05 < f < 0.30$ Hz, where f is the wave frequency) is conserved in the absence of generation and dissipation. The large reduction in energy flux observed across the array (more than 70% when waves were approximately 1 m high at the most offshore sensor (day 22 in Figure 1c)) signifies strong dissipation of the wave field.

[7] The observed dissipation rate, defined as $\kappa = -F_x/F$, where the subscript x denotes differentiation with respect to the direction of wave propagation (parallel to the array of sensors), was depth (h) dependent, increasing approximately as $h^{-3.4}$ (Figure 2) as waves propagated into shallower water.

[8] The increase of the dissipation rate with decreasing depth may explain why the coast of Kerala offers protection for fishing (and for the 15th century Portuguese fleet

[1]Woods Hole Oceanographic Institution, Woods Hole, Massachusetts, USA.

0094-8276/08/2008GL033245$05.00

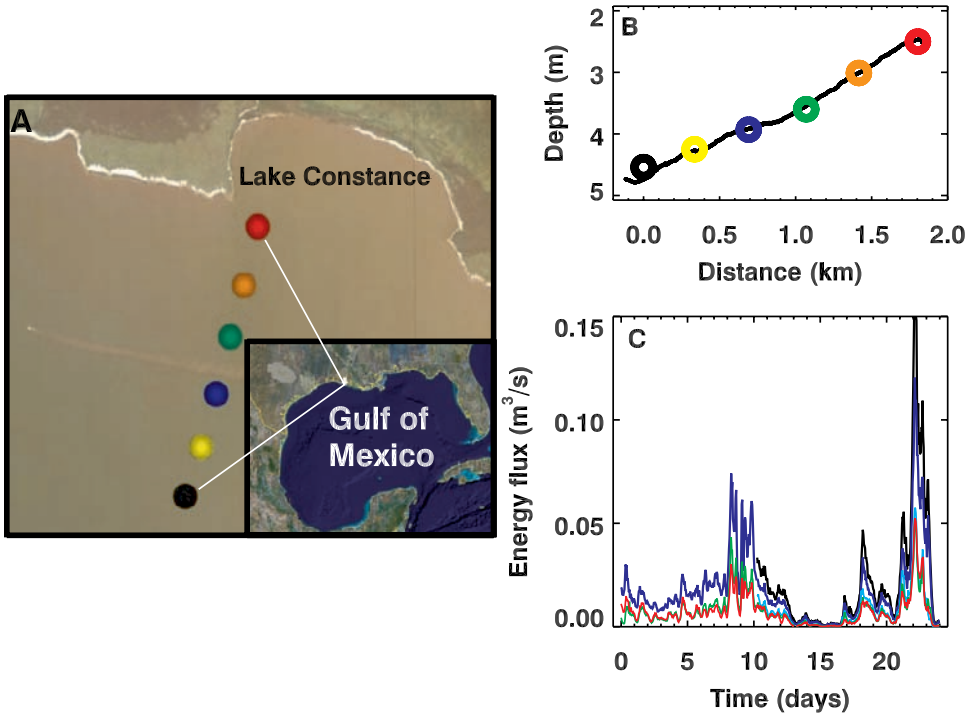

Figure 1. (a) Sensor locations (colored symbols) superposed on an aerial photo of the Louisiana coast (inset shows location within the Gulf of Mexico). (b) Depth of the seafloor (curve, estimated from a shipboard survey 100 m west of the sensors) and locations of colocated pressure gages and acoustic Doppler velocimeters (symbols) *versus* distance from the deepest (black circle) sensors. (c) Energy flux (integrated over the frequency range $0.05 < f < 0.30$ Hz) *versus* time (days since Mar 23, 2007). The black (distance = 0 km in Figure 1b), blue (distance = 0.7 km), and red (distance = 1.8 km) curves are observed energy fluxes. The turquoise and green curves are energy fluxes predicted by the dissipative Boussinesq model at the shallowest sensor (distance = 1.8 km) initialized with observations at distances = 0 and 0.7 km, respectively. If the model were perfect, the turquoise and green curves would overlay the red curve. The Boussinesq model was initialized with 51-min-long time series of sea-surface elevation estimated from the observations of near-bottom pressure corrected for water column attenuation using linear theory.

[*Pazhama*, 1996]) only after large waves and strong currents at the start of the monsoon move the mud banks from about 5- to 2-m water depth [*Nair*, 1988].

[9] Although wavenumbers (k) in shallow water ($kh < 1$) are a function of the water depth [the dispersion relationship is $f \propto k \tanh(kh)$], theoretical models for the dissipation rate that include a wavenumber dependence and the effect of increasing wave-induced pressure in shallow water [*Gade*, 1958; *Mei and Liu*, 1973; *Dalrymple and Liu*, 1978; *Yamamoto et al.*, 1978; *MacPherson*, 1980; *Hsiao and Shemdin*, 1980; *Mei and Liu*, 1987; *Liu and Mei*, 1989; *Jiang and Mehta*, 1995, 1996; *Ng*, 2000; *Lee et al.*, 2002] underpredict the observed strong increase in dissipation with decreasing depth.

3. Numerical Model Simulations

[10] Nonlinear interactions can transfer energy between waves with different frequencies [e.g., *Freilich and Guza*, 1984; *Elgar and Guza*, 1985a], so differences in energy fluxes at particular wave frequencies observed between spatially separated locations might be owing to nondissipative nonlinear energy transfers, as well as to mud-induced dissipation. Thus, to estimate the frequency dependence of the dissipation rate, the observations are compared with simulations from a nondissipative nonlinear Boussinesq wave model [*Freilich and Guza*, 1984; *Elgar and Guza*, 1985a; *Herbers et al.*, 2000] that describes waves propagating in shallow water. The numerical model was initialized with observations at each sensor and integrated to the next sensor shoreward. Differences between nondissipative model predictions and observations are attributed to dissipation in the observations. Winds were light, and are neglected, as are possible sources of dissipation (e.g., white capping) other than that induced by the muddy seafloor. The model assumes waves propagate along the sensor array (with small directional spread) and reflections from the shoreline are small, consistent with wave directional spectra estimated with the colocated pressure and velocity time series. Accumulation of model errors is reduced by reinitializing the model with observations at each sensor and integrating only to the next sensor shoreward. A similar approach has been used to estimate the frequency-dependent dissipation caused by breaking in the surfzone [*Kaihatu and Kirby*, 1995; *Elgar et al.*, 1997; *Herbers et al.*, 2000].

[11] The comparisons of the observations with Boussinesq model predictions suggest dissipation rates are highest for relatively low frequency "infragravity" motions (f = 0.07 Hz in Figure 3a). In contrast to dissipation functions developed for two-layer systems consisting of water overlying a 0.3-m-thick layer of fluid mud with density 1.3g/cm^3 [*Gade*, 1958; *Mei and Liu*, 1973; *Dalrymple and Liu*, 1978;

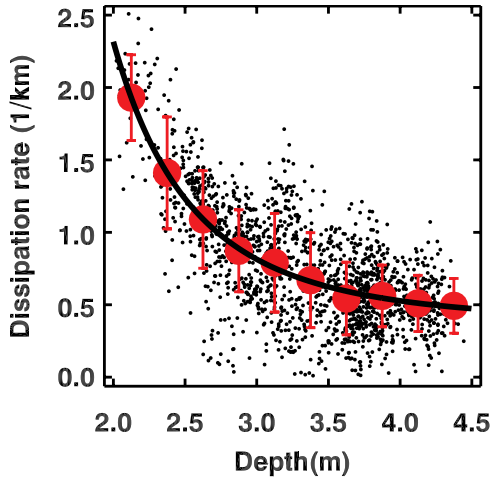

Figure 2. Overall ($0.05 < f < 0.30$ Hz) dissipation rate estimated from differences in energy fluxes observed at neighboring sensor locations. The tidal range was approximately 1 m, providing a wide range of depths. Black dots are dissipation rates from 51-min-long data runs (sampled at 2 Hz), and red circles (vertical bars are ± 1 standard deviation) are averages within 0.25-m-wide depth bins. The black curve is a least squares fit through the 1571 unbinned data points (results are similar if the bin-averaged values (red symbols) are used), such that dissipation rate $\kappa = 23\mathrm{h}^{-3.4} + 0.3$.

Yamamoto et al., 1978; *MacPherson*, 1980; *Hsiao and Shemdin*, 1980; *Mei and Liu*, 1987; *Liu and Mei*, 1989; *Jiang and Mehta*, 1995, 1996; *Ng*, 2000; *Lee et al.*, 2002], and to functions commonly used in numerical wave models [*Wintertwerp et al.*, 2007; *Kaihatu et al.*, 2007], the maximum dissipation rate estimated here (Figure 3a) occurs for relatively low frequencies (equivalently, for long wavelengths such that $0.2 < kh < 0.3$ *versus* $kh \approx 1$ [*Kaihatu et al.*, 2007]). During these observations, the 0.3-m-thick layer of dense mud that covered the seafloor along the sensor transect was able to resist shear, and thus was not fluid, suggesting that theories must account for different rheological behavior for the situation here.

[12] An empirical formula that accounts for both the depth and frequency dependence of the estimated dissipation rate was determined by a least squares fit to the estimated dissipation functions (Figure 3a). When extended to account for mud-induced dissipation by including the empirical function, the (dissipative) Boussinesq model reproduces the evolution of the wave field for a wide range of conditions (Figure 4).

[13] The fidelity of the 1.8-km-long model simulations (Figures 1c and 4) suggests that the technique used to estimate the dissipation function is not corrupted by potential errors associated with integrating the nondissipative Boussinesq model over the ≈ 0.35-km distances between the sensors (where there is dissipation) before reinitializa-

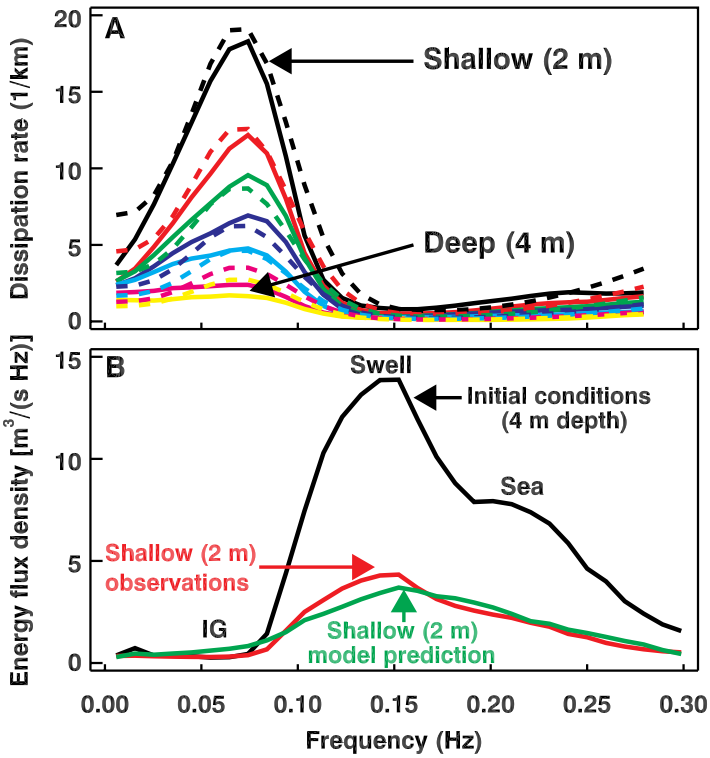

Figure 3. (a) Dissipation rate *versus* frequency. Solid curves are differences between the nondissipative Boussinesq model and the observations averaged over all 51-min-long runs in 0.3-m wide depth bins from approximately 4 (yellow) to 2 m (black) depth. The dashed curves are based on a least squares fit (of a Gaussian function combined with a quadratic) to the solid curves that accounts for the observed $h^{-3.4}$ depth dependence, and are given by: $\kappa = 31h^{-3.4}[6.2 \exp\{-1/2((f-0.07)/0.03)^2\}] + 2.5 - 27f + 82f^2$ (b) Energy flux density *versus* frequency observed at the deepest (≈ 4 m depth, black curve) and shallowest (≈ 2 m depth, red) sensors, and predicted by the dissipative Boussinesq model in 2 m depth (green). The model was initialized with the ≈ 1 m high waves observed in 4 m depth between 0300 and 0351 hrs CST Apr 14, 2007 (day 22 in Figure 2).

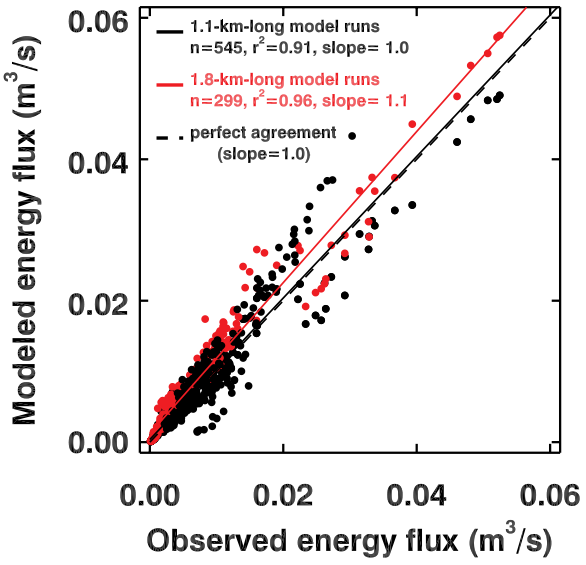

Figure 4. Energy flux predicted by the dissipative Boussinesq model *versus* energy flux estimated from the observations at the shallowest sensor. The Boussinesq model was initialized with observations from the sensors located at distance = 0 (red symbols) and distance = 0.7 km (black symbols), 1.8 and 1.1 km offshore of the shallowest sensor (distance = 1.8 km), respectively (Figure 1). Linear least squares fits through the points based on 1.8- (red line) and 1.1- (black line) km-long model integrations have slopes (1.0 and 1.1, respectively) close to 1 (dashed line), with correlations of $r^2 = 0.96$ (299 points) and 0.91 (545 points), respectively.

tion. Although the model results are consistent with the observations, there is some scatter (Figure 4), possibly because of (small) violations of the assumptions of light winds, no white capping, and waves propagating along the sensor array with no directional spread.

[14] For a case study with the largest waves (1 m significant wave height) measured at the deepest sensor, the dissipative Boussinesq model predicts the observed 70% reduction in overall energy flux (day 22 in Figure 1c), as well as details of the energy flux spectrum (Figure 3b). In particular, the model predicts that near-resonant nonlinear interactions between high-frequency sea ($f = 0.22$ Hz) and mid frequency swell ($f = 0.15$ Hz) transfer energy to lower frequency ($f = 0.07$ Hz) infragravity motions where the dissipation rate is highest (Figure 3a). Bispectral analysis [*Elgar and Guza*, 1985b] of the observations and the model simulations suggests that these are difference interactions, similar to the transfer of energy from groups of swell waves to lower frequency motions [*Elgar and Guza*, 1985b; *Kaihatu and Kirby*, 1995; *Elgar et al.*, 1997; *Herbers et al.*, 2000]. As the wave field propagates into shallower water, these interactions between relatively high frequency waves and infragravity motions become stronger [*Freilich and Guza*, 1984; *Elgar and Guza*, 1985a, 1985b; *Kaihatu and Kirby*, 1995; *Elgar et al.*, 1997; *Herbers et al.*, 2000], transferring more energy to motions where dissipation rates are high. The resulting reduction of energy levels occurs across a wide range of frequencies, including waves that are in relatively deep water ($kh \approx 1$), and thus are not expected to interact directly with the seafloor. The increase in nonlinear transfers of energy to motions where dissipation rates are high as the waves shoal may explain why dissipation increases rapidly with decreasing depth, and thus why waves near Kerala are attenuated strongly only when the mud banks have migrated into shallow water after the monsoons begin.

[15] Mild-slope equation-based numerical simulations of simplified wave fields propagating in a two-layer fluid [*Kaihatu et al.*, 2007] in deeper water ($kh \geq 1$) where the nonlinear interactions are not resonant are consistent with the results presented here, suggesting the mechanism of nonlinear energy transfers from high frequency waves combined with dissipation of low frequency motions may attenuate waves for a range of water depths.

[16] The observations presented here are consistent with the hypothesis [*Sheremet and Stone*, 2003; *Kaihatu et al.*, 2007] that as low frequency infragravity energy is dissipated by the mud, additional energy is transferred from higher frequency motions (some of which have wavelengths too short to interact directly with the seafloor). As the waves propagate into shallower water, the nonlinear interactions approach resonance, allowing large and rapid transfers of energy from sea and swell to lower-frequency infragravity motions [*Freilich and Guza*, 1984; *Elgar and Guza*, 1985a, 1985b; *Kaihatu and Kirby*, 1995; *Elgar et al.*, 1997; *Herbers et al.*, 2000] where dissipation rates are maximum. The combination of low-frequency dissipation and nonlinear energy transfers from higher-frequency waves results in reduction of energy across a wide frequency range.

[17] **Acknowledgments.** We thank A. Sheremet, A. Mehta, and G. Kineke for discussions, G. Kineke and S. Bentley for sharing results from their shipboard surveys, and L. Gorrell, W. Boyd, K. Smith, and the captain and crew of the R/V Acadiana for help gathering the field observations despite alligators, water moccasins, and unpleasant accommodations in the bayous of Louisiana. The Office of Naval Research provided support.

References

Allison, M., G. Kineke, E. Gordon, and M. Goni (2000), Development and reworking of a seasonal flood deposit on the inner continental shelf off the Atchafalaya River, *Cont. Shelf Res.*, *20*, 2267–2294.

Dalrymple, R., and P. Liu (1978), Waves over soft muds: A two-layer fluid model, *J. Phys. Oceanogr.*, *8*, 1121–1131.

Draut, A., G. Kineke, D. Velasco, M. Allison, and R. Prime (2005), Influence of the Atchafalaya River on recent evolution of the Chenier-plain inner continental shelf, northern Gulf of Mexico, *Cont. Shelf Res.*, *25*, 91–112.

Elgar, S., and R. Guza (1985a), Shoaling gravity waves: A comparison between data, linear finite depth theory, and a nonlinear model, *J. Fluid Mech.*, *158*, 47–70.

Elgar, S., and R. Guza (1985b), Observations of bispectra of shoaling surface gravity waves, *J. Fluid Mech.*, *161*, 425–448.

Elgar, S., R. Guza, B. Raubenheimer, T. Herbers, and E. Gallagher (1997), Spectral evolution of shoaling and breaking waves on a barred beach, *J. Geophys. Res.*, *102*, 15,797–15,805.

Forristall, G., and A. Reece (1985), Measurements of wave attenuation due to a soft bottom: The SWAMP experiment, *J. Geophys. Res.*, *90*, 3367–3380.

Freilich, M., and R. Guza (1984), Nonlinear effects on shoaling surface gravity-waves, *Philos. Trans. R. Soc. London, Ser. A*, *311*, 1–41.

Gade, H. (1958), Effects of a non-rigid, impermeable bottom on plane surface waves in shallow water, *J. Mar. Res.*, *16*, 61–82.

Herbers, T., N. Russnogle, and S. Elgar (2000), Spectral energy balance of breaking waves within the surf zone, *J. Phys. Oceanogr.*, *30*, 2723–2737.

Hsiao, S., and O. Shemdin (1980), Interaction of ocean waves with a soft bottom, *J. Phys. Oceanogr.*, *10*, 605–610.

Jiang, F., and A. Mehta (1995), Mudbanks of the southwest coast of India IV: Mud viscoelastic properties, *J. Coastal Res.*, *11*, 918–926.

Jiang, F., and A. Mehta (1996), Mudbanks of the southwest coast of India V: Wave Attenuation, *J. Coastal Res.*, *12*, 890–897.

Kaihatu, J., and J. Kirby (1995), Nonlinear transformation of waves in finite water depth, *Phys. Fluids*, *7*, 1903–1914.

Kaihatu, J., A. Sheremet, and T. Holland (2007), A model for the propagation of nonlinear surface waves over viscous muds, *Coastal Eng.*, *54*, 752–764.

Lee, T., J. Tsai, and D. Jeng (2002), Ocean waves propagating over a Columb-damped poro-elastic seabed of finite thickness, *Comput. Geotech.*, *29*, 119–149.

Liu, K., and C. Mei (1989), Effects of wave-induced friction on a muddy seabed modeled as a Bingham-plastic fluid, *J. Coastal Res.*, *SI5*, 777–789.

MacPherson, H. (1980), The attenuation of water waves over a non-rigid bed, *J. Fluid Mech.*, *97*, 721–742.

Mathew, J., M. Baba, and N. Kurian (1995), Mudbanks of the southwest coast of India I: Wave characteristics, *J. Coastal Res.*, *11*, 168–178.

Mei, C., and P. Liu (1973), The damping of surface gravity waves in a bounded fluid, *J. Fluid Mech.*, *59*, 239–256.

Mei, C., and P. Liu (1987), A Bingham-plastic model for a muddy seabed under long waves, *J. Geophys. Res.*, *92*, 14,581–14,594.

Nair, A. (1988a), Mudbanks (chakara) of Kerala—A marine environment to be protected, paper presented at National Seminar on Environmental Issues, Univ. of Kerala, Trivandrum, India.

Ng, C. (2000), Water waves over a muddy bed: A two layer Stokes' boundary layer model, *Coastal Eng.*, *40*, 221–242.

Pazhama, H. G. K. (1996), *Dr. Herman Gundardt Kerala Pazhama,* translated by T. Krishnan, Mathrubhumi, Kochi, India.

Sheremet, A., and G. W. Stone (2003), Observations of nearshore wave dissipation over muddy sea beds, *J. Geophys. Res.*, *108*(C11), 3357, doi:10.1029/2003JC001885.

Wells, J., and J. Coleman (1981), Physical processes and fine-grained sediment dynamics, coast of Surinam, South-America, *J. Sediment. Petrol.*, *51*, 1053–1068.

Wintertwerp, J., R. de Graaff, J. Groeneweg, and A. Luijendijk (2007), Modelling of wave damping at Guyana mud coast, *Coastal Eng.*, *54*, 249–261.

Yamamoto, T., H. Koning, H. Sellmeijer, and E. van Hijum (1978), On the response of a poro-elastic bed to water waves, *J. Fluid Mech.*, *87*, 193–206.

S. Elgar, Woods Hole Oceanographic Institution, MS11, Woods Hole, MA 02543, USA. (elgar@whoi.edu)

B. Raubenheimer, Woods Hole Oceanographic Institution, MS12, Woods Hole, MA 02543, USA. (britt@whoi.edu)